Experimental Study on Base Drag Reduction with Combined Lateral and Axial Injection

K. C. Schadow* and D. J. Chieze†
Naval Weapons Center, China Lake, Calif.

Experiments have been performed in a two-dimensional (2D), planar Mach 2 wind tunnel to study injection and combustion processes around a simulated projectile base. Lateral injection and external burning (EB) of hot fuel-rich reaction products from solid propellants, axial base injection (BI) of helium and nitrogen, and combined EB and BI have been studied. Test results show that the two base pressure rise mechanisms associated with EB and BI can be superimposed. Moreover, the base pressure rise associated with combined EB and BI was found to be higher than with EB or BI alone.

Nomenclature

A = area
BB = base burning with axial fuel injection through projectile base into viscous near-wake region
BI = base injection through projectile base without combustion
c_D = discharge coefficient
D = diameter
EB = external burning in inviscid flow region achieved by lateral supersonic injection velocity
EB/BR = external burning/base reaction achieved by lateral subsonic injection velocity
h = base height
I = injection parameter $= \dot{m}_j / u_1 \rho_1 A_b$
I_{sp} = specific impulse $= \Delta p_b A_b / \dot{m}_j$
M = Mach number
$\dot{m}$ = mass flow
p = static pressure
RSP = rear stagnation point
u = axial velocity component
T = temperature
X = axial coordinate measured from base
α = corner flow turning angle
Δp = pressure rise due to injection and/or combustion
κ = ratio of specific heats
ρ = density

Subscripts

1 = condition before base corner expansion
b = base
b(ax) = in connection with Δp: base pressure rise due to axial injection in tests with EB and BI [$\Delta p_{b(ax)}$ = (Δp_b with BI and EB) − (Δp_b with EB)]
PM = primary motor
j = injector
ax = axial
lat = lateral
tot = total (in connection with I: $I_{tot} = I_{ax} + I_{lat}$)
t = total (in connection with p: total pressure as determined with pressure probe)
$t(PM)$ = throat (primary motor)

Presented as Paper 78-25 at the AIAA 16th Aerospace Sciences Meeting, Huntsville, Ala., Jan. 16-18, 1978; submitted Feb. 10, 1978; revision received May 30, 1978.

Index categories: Reactive Flows; Airbreathing Propulsion.

*General Engineer, Aerothermochemistry Division.
†Engineering Technician, Aerothermochemistry Division.

Introduction

THE base pressure of a projectile traveling at supersonic speed can be controlled by burning a fuel near the base region. Specifically, the base pressure can be raised closer to freestream pressure (to reduce drag) or may be raised above freestream pressure (to provide propulsion). Two methods have been investigated and discussed in the literature: base burning with axial subsonic fuel injection through the projectile base into the subsonic, viscous near-wake region (Fig. 1a), and external burning outside the near-wake region with lateral supersonic fuel injection into the supersonic inviscid flow region (Fig. 1b).

Base pressure alteration by base burning of hydrogen has been studied by Baker et al.[1] and Townsend and Reid.[2] It was found that the base pressure could be raised close to static freestream pressure, which corresponds to base drag elimination.

Base burning using solid propellants has been studied recently by Andersson et al.[3] In Andersson's free-flight tests with 105- and 120-mm projectiles, base drag reduction of up to 70% at a specific impulse of up to $I_{sp} = 580$ s has been demonstrated.

General experience shows that the maximum base pressure rise attainable with base burning is limited. The following simplified consideration shows that, under practical injection conditions, a base pressure higher than freestream pressure, and therefore propulsion, cannot be achieved. As shown in Fig. 1a, the airflow surrounding a projectile at supersonic flight turns and expands around the base corner at a turning angle α, so that the air freestream pressure after expansion matches the pressure in the near-wake region. The turning angle α is largest (and the base pressure lowest) without base burning. When mass and heat addition into the base region occurs, the base pressure rises and the base region is extended, which reduces the turning angle α. Reduction of α, however, is limited to zero. Under these conditions, airflow turning and expansion around the base corner is eliminated, and the base pressure reaches the highest value, namely, the freestream pressure. In the following, base burning in the subsonic near wake region achieved by axial fuel injection will be symbolized by BB.

With the external burning concept, a propulsion mode is theoretically possible, because the energy release in the inviscid region outside the viscous base region can generate and contain a base pressure higher than the freestream pressure, as shown by Strahle[4] and Mehta and Strahle.[5] These analytical studies also have predicted that the base region is shortened or compressed by the combustion waves impinging on the base region. A compression of the base region has been demonstrated experimentally in wind tunnel tests with simulated

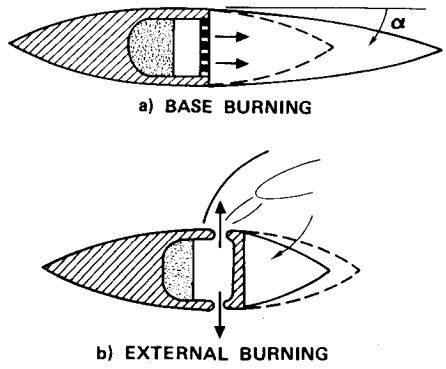

Fig. 1 Two methods of base pressure alteration.

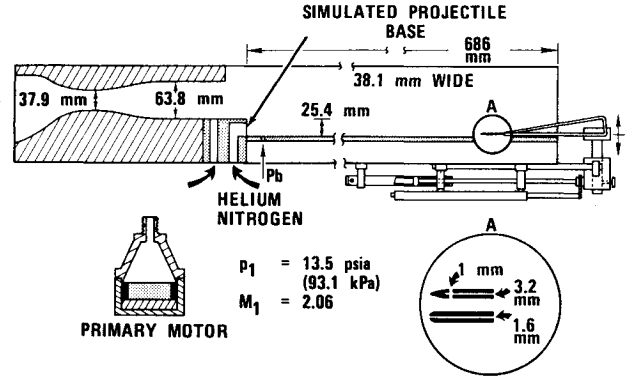

Fig. 2 Test setup.

external burning disturbances (no combustion) by Neale et al.[6] and with external burning of fuel-rich solid propellant reaction products by Schadow and Chieze.[7] The base pressure rise associated with the compression of the base region has not been significiant in Schadow's test. Only 40% of the base pressure rise necessary for base drag elimination has been achieved. Schadow's tests have been performed in a 2D, planar wind tunnel in which the external burning environment has been simulated successfully, as demonstrated by detailed flow measurements.[7] If these 2D, planar wind tunnel tests are indicative of the performance of full-scale external burning-assisted projectiles, it must be expected that the external burning concept, as shown in Fig. 1b, will not produce the high base pressures theoretically predicted. In the following, external burning with lateral supersonic injection velocity and with negligible reaction in the viscous, subsonic near-wake region is symbolized by EB.

In addition to BB and EB, base pressure rises can be achieved by the combination of BB and EB. This method, which was suggested for the first time by Townend,[8] has not been studied experimentally in detail. Some experimental evidence exists suggesting that reaction in the subsonic base region, in addition to EB, may be promising to achieve optimum base pressure rise. Schadow and Chieze[7] have reduced the lateral injection velocity from supersonic to subsonic speed, partly to inject the fuel-rich reaction products through the projectile boundary layer into the supersonic flow region, and partly to entrain them via the projectile boundary layer into the subsonic base region. Two results were found in the tests with subsonic injection velocity: 1) at the same time, supersonic EB and reaction in the region have been achieved; and 2) the base pressure rise has been significantly higher than with EB alone. In the following, a concept with subsonic lateral injection velocity, which produces external burning with significant reaction in the base region (base reaction), will be symbolized as EB/BR.

It can be speculated that the highest base pressure rises can be achieved when, in addition to EB, reaction in the near-wake region is supplemented by axial fuel injection (base burning). With such a combined EB and BB concept, it may be possible to achieve a propulsion mode, when the base pressure is raised close to freestream pressure by BB and then raised further above freestream pressure by EB. If such a concept is at all feasible, it has to be demonstrated that the two base pressure rise mechanisms of EB (compression of base region) and BB (elongation of base region) can be superimposed. Only then can it be expected that the base pressure rise resulting from combined EB and BB will be the sum of the base pressure rises attainable with EB and BB alone.

The objective of the tests described in this paper was to investigate experimentally the two mechanisms of EB and BB and to determine if they can be superimposed. To simplify the experiments, BB was substituted by axial subsonic base injection (in the following symbolized by BI) of nitrogen and helium. This substitution is possible, since the base pressure rise mechanism is the same for BB and BI. In both cases, the base pressure rise is associated with an extension of base region or a decrease of the airflow turning angle. Two types of experiments were performed. First, the length of the base region was determined for 1) BI of helium and nitrogen, 2) EB using fuel-rich solid propellants, and 3) the combination of BI and EB. If superimposing of EB and BI is possible, it must be expected that the base region will be elongated during BI and then compressed during superimposed EB. Second, the base pressure rise was determined for the three injection conditions. If superimposing is possible, it must be expected that the base pressure rise with combined BI and EB will be nearly the sum of the base pressure rises possible with EB and BI alone.

In the previously described tests, BI was combined with EB with lateral *supersonic* injection. Tests also were made where BI was combined with EB/BR with lateral *subsonic* velocity. In this case, some of the laterally injected fuel might be entrained into the base region via the projectile boundary layer.

The experiments were performed in a 2D, planar wind tunnel in which the BI and EB environment was simulated. Detailed flow measurements have shown[7] that base pressure measurement without measureable tunnel interference can be performed. Specifically, it was determined that 1) at airflow-only conditions (no combustion), the base pressure and centerline pressure distribution were in acceptable agreement with theoretical predictions; 2) at airflow-only conditions, simulated injection shocks, which were produced by a flow obstruction in the base corner approach flow, did not interfere with the base pressure measurement; and 3) at external burning conditions, the near-wake closure point was located inside the wind tunnel, and the combustion zone outside the near-wake region was supersonic, thus precluding communication between the base region and the ambient pressure conditions outside the wind tunnel.

Test Setup

The planar, 2D wind tunnel is shown in Fig. 2. The air entered the 38.1-mm-wide test section from the left and expanded to a Mach 2.06 airstream of 13.5 psia (93.1 kPa) freestream pressure and ambient temperature, as experimentally determined in Ref. 7. The simulated projectile base (base height = 25.4 mm) was located at the downstream end of the Mach 2 nozzle. Downstream of the simulated base, the wind tunnel was open at the top to allow free expansion and closed at the bottom. The bottom tunnel wall represented the centerline of the base region.

The shaded area of Fig. 2 includes the injectors of axial and lateral injection and the connection to the primary motor with the fuel-rich propellants and to the helium and nitrogen feed system. Details of the shaded area are shown in Fig. 3.

For supersonic lateral injection velocity, an injector with $D_{j,\mathrm{lat}} = 5.1$ mm diam was used. For subsonic lateral injection velocity, a double-throat arrangement with $D_{j,\mathrm{lat}} = 10.2$ mm ϕ

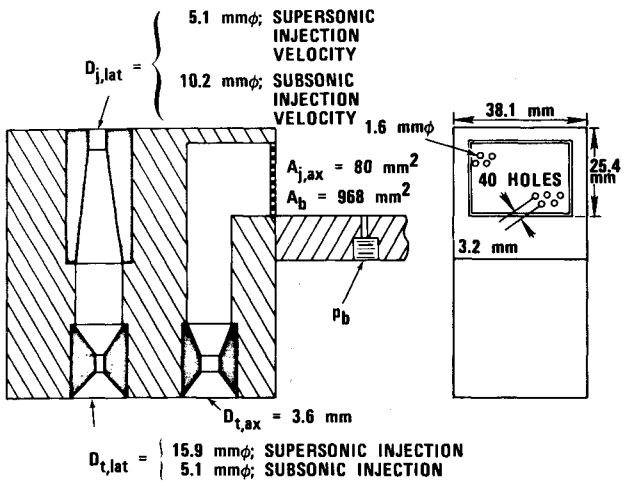

Fig. 3 Geometries for axial and lateral injection.

and $D_{t,lat} = 5.1$ mm ϕ was used. Helium and nitrogen were injected axially through a plate with 40 holes, each of 1.6 mm ϕ. The entire injection area was 80 mm^2. To achieve subsonic injection velocity, an orifice of $D_{t,ax} = 3.6$ mm was placed into the feed system, which also included an orifice meter for mass flow measurement.

In the primary motor, a fuel-rich solid propellant with hydroxyl-terminated polybutadiene (HTPB), ammonium perchlorate (AP), magnesium, and boron was used. The 61-mm ϕ end-burning grain delivered a mass flow of about $\dot{m}_{j,lat} = 0.018$ kg/s at a primary chamber pressure of $p_{PM} = 160$ psia (1.1×10^3 kPa).

The axial and lateral injectant mass flow was characterized by the axial injection parameter I_{ax} and the lateral injection parameter I_{lat}. The sum of I_{ax} and I_{lat} was the total injection parameter I_{tot}. The injection parameter was calculated to

$$I = \frac{\dot{m}_j}{\rho_l u_l A_b} = \frac{\dot{m}_j}{p_l A_b M_l \sqrt{(\kappa \text{ mol wt})/RT_l}}$$

With $M_l = 2.06$, $p_l = 13.5$ psia (93.1 kPa), $T_l = 276$ K, and $A_b = 38.1$ mm (tunnel width) $\times$ 25.4 mm (base height), the injection parameter was calculated to $I = \dot{m}_j$ (kg/s)/0.78 (kg/s).

Experimental methods consisted of total and static pressure measurements, p_t and p, using a movable probe system (Fig. 2), and base pressure measurement p_b at a location one base height ($X/h = 1$) downstream of the base (see Figs. 2 and 3). Because of near zero velocity in the base region, it can be assumed that the base region pressure at $X/h = 1$ will be the same as at the base at $X/h = 0$.

With the movable pressure probes, the length of the base region, characterized by the near stagnation point (RSP), was determined for the various injection conditions. To determine the location of RSP, where the centerline velocity starts to increase from near zero to supersonic speed, the pressure probes were positioned as close as possible to the bottom wall of the wind tunnel. In this position, which was 1.6 mm above the tunnel wall, the probes were moved from the base into downstream direction. RSP is located at the position where p_t started to exceed p. Two examples are given in Fig. 4, which shows p_t and p as a function of X/h, the normalized axial distance downstream of the base, for test 6 with helium BI and test 18 with helium BI and EB/BR. It may be seen that, in these tests, the RSP was located at $X/h = 4.45$ (test 6) and 10.3 (test 18), where p_t started to exceed p.

Before the experimental program was performed, data accuracy of the pressure measurements with variable capacitance transducers was determined to be $\pm 2\%$. This error includes the inaccuracy of the manual evaluation of the

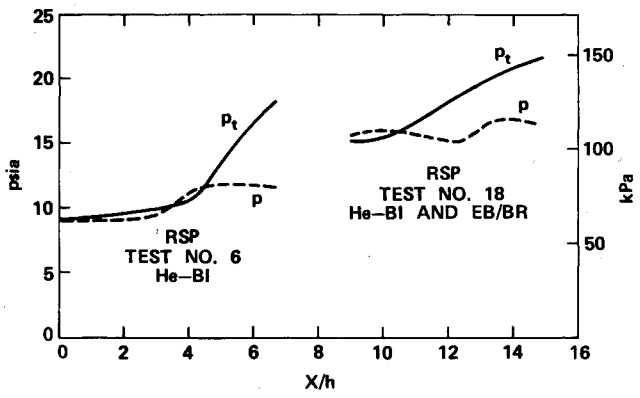

Fig. 4 Determination of RSP.

oscillograph records. The accuracy of injectant mass flow $\dot{m}_{j,ax}$, which was measured with an orifice meter, was determined to be $\pm 5\%$. This error was estimated from the uncertainties in orifice diameter, flow coefficient, and expansion factor. The propellant mass flow $\dot{m}_{j,lat}$ was measured within $\pm 6\%$ with

$$\dot{m}_{j,lat} = p_{PM} A_{t(PM)} c_D$$

This large error mainly resulted from uncertainties of determining the discharge coefficient c_D ($\pm 3.5\%$). The accuracy of determining the position of RSP was estimated to be $\pm 5\%$ due to possible errors in the p and p_t measurements. Effects of pressure lag due to line volume on p and p_t measurements were eliminated by determining a minimum travel rate of the probe.

Repeatability of base pressure measurement and determination of the position of RSP was checked in a series of six tests without combustion. Maximum deviation of any result from the mean result from this series of tests was found to be less than $\pm 3\%$ for the base pressure and $\pm 2\%$ for the position of the RSP.

Test Matrix

A total of 20 wind tunnel tests were conducted. For each test, the following parameters were determined: base pressure (p_b), and base pressure rise (Δp_b), the normalized base pressure rise ($\Delta p_b/p_l$), injectant mass flows ($\dot{m}_{j,ax}$ and/or $\dot{m}_{j,lat}$), injection parameter (I_{ax} and/or I_{lat}, and, if applicable, I_{tot}), and the location of RSP.

Tests were made at eight different test conditions:

1) Airflow-only condition without injection (test 1) to determine the reference base pressure and location of RSP for the following tests with injection and combustion.

2) Nitrogen BI with three different injectant mass flows (tests 2-4).

3) Helium BI with six different injectant mass flows (tests 5-10).

4) EB with supersonic lateral injection (test 11).

5) EB/BR with subsonic lateral injection (test 12).

6) Combined EB and nitrogen BI at three different nitrogen mass flows (tests 13-15).

7) Combined EB and helium BI at two different helium mass flows (tests 16 and 17).

8) Combined EB/BR and helium BI with three different helium mass flows (tests 18-20).

Test Results

Two types of test results will be reported which will show whether the two mechanisms of BI and EB can be superimposed. These results are the position of the RSP and the base pressure rise during the different injection and combustion conditions. The results will be presented in the following order: 1) air-only condition, 2) independent BI, EB, and

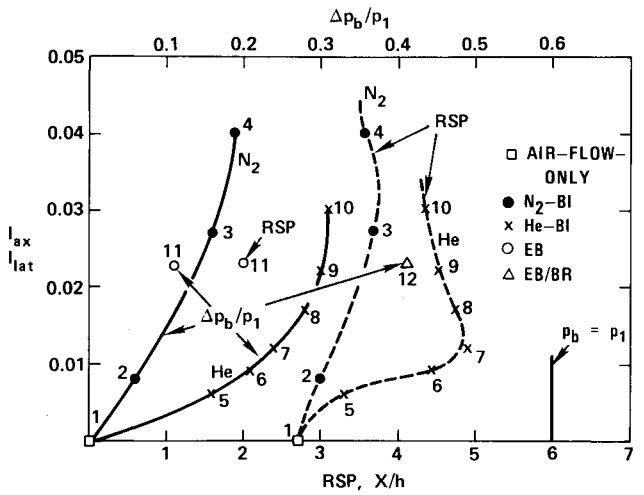

Fig. 5 Base pressure rise $\Delta p_b/p_1$ and location of RSP as a function of injection parameter I.

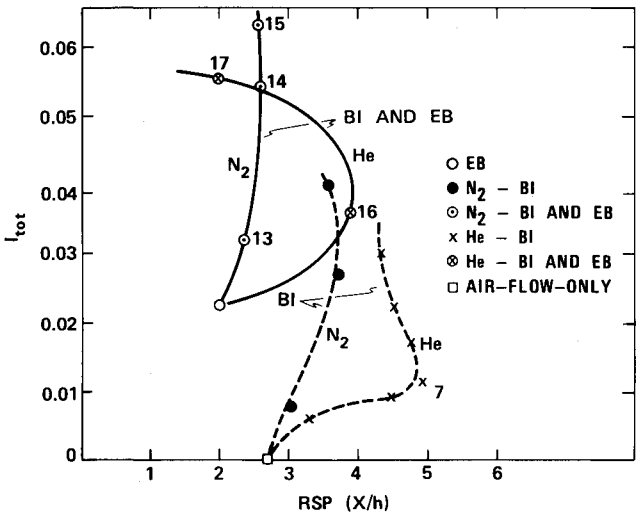

Fig. 6 Location of RSP as a function of injection parameter.

EB/BR, 3) combined BI and EB, and 4) combined BI and EB/BR.

Airflow-Only Condition

At this reference condition for the following injection and combustion tests, the RSP was located at $X/h = 2.7$ (test 1). The pressure in the base region was $p_b = 5.4$ psia (37.3 kPa).

BI; EB; EB/BR

The RSP and Δp_b results for these conditions are summarized in Fig. 5. In this figure, the injection parameters for axial injection I_{ax} and for lateral injection I_{lat} are shown on the vertical coordinate. The scale for X/h for the location of RSP is shown on the lower horizontal coordinate, while the scale for the normalized base pressure rise $\Delta p_b/p_1$ is shown in the top horizontal coordinate. As indicated in the figure, a pressure rise of $\Delta p_b/p_1 = 0.6$ is needed to achieve a base pressure p_b equal to the freestream pressure p_1.

With BI, the RSP moved downstream from its position at $X/h = 2.7$ without injection and approached with increasing injection parameter a downstream position that depended on the type of injectant. With nitrogen injection, RSP moved to $X/h = 3.55$ at $I_{ax} = 0.040$ (see dotted line for tests 2-4 in Fig. 5); with helium injection, RSP moved to $X/h = 4.35$ at $I_{ax} = 0.029$ (see dotted line for tests 5-10). These RSP test results showed that the base region extension through BI was

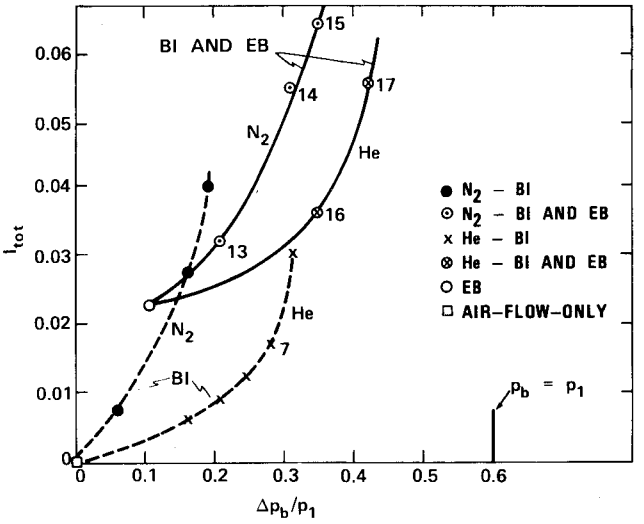

Fig. 7 Base pressure rise $\Delta p_b/p_1$ as a function of injection parameter.

limited. The tests also showed that the base pressure rise attainable with BI was limited. As may be seen from the solid lines in Fig. 5, the base pressure rise approached $\Delta p_b/p_1 = 0.19$ with nitrogen injection (tests 2 to 4) and $\Delta p_b/p_1 = 0.31$ with helium injection (tests 5-10).

With EB, RSP moved upstream to $X/h = 2.0$, corresponding to a compression of the near-wake region. The compression caused a base pressure rise of $\Delta p_b/p_1 = 0.11$ (see circles for test 11 in Fig. 5). With EB/BR, RSP moved downstream to $X/h = 10.5$ (not shown in Fig. 5) with $\Delta p_b/p_1 = 0.41$ /(triangle for test 12 in Fig. 5).

Combined BI and EB

The tests showed that a base region extended by BI could be compressed when EB was superimposed. This is demonstrated in Fig. 6, which shows the position of RSP vs I_{tot} for combined nitrogen BI and EB (tests 13-15) and combined helium BI and EB (tests 16 and 17). For both nitrogen and helium as injectants, RSP with combined EB and BI (solid lines) was located further upstream than BI alone (dotted lines). The results for combined EB and BI in Fig. 6 are based on I_{tot}, which was calculated from axially and laterally injected mass flows.

The base pressure rise during combined EB and BI was higher than with BI alone, as seen in Fig. 7, which shows $\Delta p_b/p_1$ vs I. A comparison of combined EB and BI (solid lines) and BI alone (dotted lines) shows that, for nitrogen injection, superimposed EB increased the base region pressure rise by $\Delta p_b/p_1 = 0.16$ maximum (tests 13-15) and for helium injection by $\Delta p_b/p_1 = 0.11$ (tests 16 and 17).

Combined BI and EB/BR

For this combination, the RSP was located at $X/h = 10.5$ (see RSP curve for tests 18-20 in Fig. 8). This location was independent of the helium injection parameter and was the same as for EB/BR alone (test 12). The base pressure rise during combined BI and EB/BR was higher than with BI alone and approached $\Delta p_b/p_1 = 0.6$ (see $\Delta p_b/p_1$ curve for tests 18-20 in Fig. 8). With this pressure rise, the base region pressure is equal to freestream pressure, and base drag is eliminated. The base pressure rise, which was achieved with combined BI and EB/BR, was less than the sum of the pressure rises that were achieved with BI and EB/BR alone. For example, in test 20 with combined BI and EB/BR, the pressure rise was $\Delta p_b/p_1 = 0.58$, which is less than the sum of $\Delta p_b/p_1 = 0.31$ with BI at the same I_{ax} (test 10) and $\Delta p_b/p_1 = 0.41$ with EB/BR (test 12).

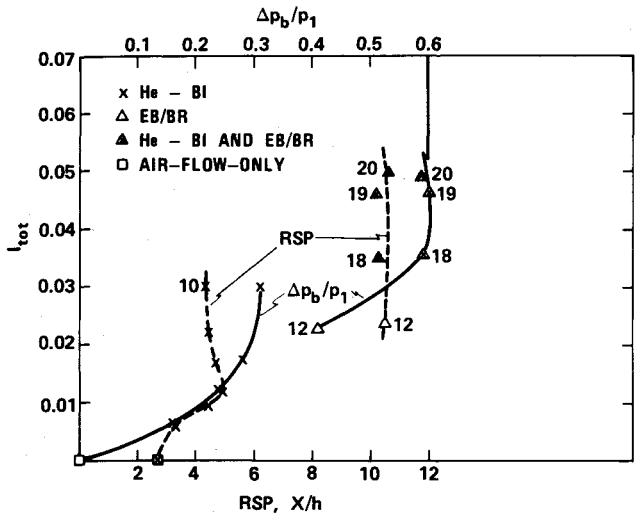

Fig. 8 Base pressure rise $\Delta p_b/p_l$ and location of RSP as a function of injection parameter.

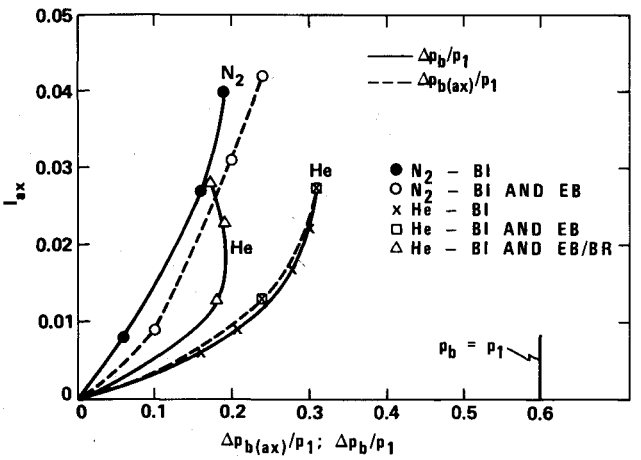

Fig. 9 Base pressure rise due to axial injection $\Delta p_{b(ax)}/p_l$ as a function of injection parameter.

A summary of the test results is given in Fig. 9. In this figure, $\Delta p_b/p_l$ for BI is compared with $\Delta p_{b(ax)}/p_l$ for BI and EB (EB/BR). The $\Delta p_{b(ax)}/p_l$, which is the base pressure rise component due to axial injection in these tests with combined BI and EB (EB/BR), was calculated from the base pressure rise difference of Δp_b with BI and EB (EB/BR) minus Δp_b with EB (EB/BR). The figure directly shows that BI and EB can be superimposed. With helium, $\Delta p_{b(ax)}/p_l$ in tests with BI and EB was essentially equal to $\Delta p_b/p_l$ with BI alone. With nitrogen, $\Delta p_{b(ax)}/p_l$ was even greater than $\Delta p_b/p_l$, indicating that Δp_b due to axial injection is greater with superimposed EB than with BI alone. Figure 9 also directly shows that superimposition of the base pressure rise is not possible with the combination of BI and EB/BR.

Discussion

An experimental program was undertaken to determine whether the base pressure rise mechanisms of EB (characterized by a compression of the base region) and BI (characterized by an extension of the base region) can be superimposed. The test results show that both mechanisms can be superimposed, and, by this means, higher base pressure can be achieved than with each mechanism alone. Superimposition of EB and BI was demonstrated by determining the position of the RSP with BI, EB, and combined BI and EB. The tests with helium and nitrogen BI described in Fig. 6 showed that the base region (characterized by the RSP) was elongated by BI and then compressed when EB was superimposed. The net effect was an elongation of the base region. The base pressure rise, resulting from the combination of both mechanisms, was the sum (and more) of the pressure rises achieved with BI and EB alone, as described in Fig. 7. To achieve optimum pressure rise with the combination of EB and BI, it is necessary to achieve highest pressure rises by BI and EB alone.

The base pressure rise for BI strongly depends on the molecular weight of the injectant. The molecular weight should be as low as possible. The tests showed that the pressure rise was significantly higher with helium (mol. wt. = 4) than with nitrogen (mol. wt. = 28) at the same injection parameters. For example, for $I_{ax} = 0.03$, the base pressure rise was $\Delta p_b/p_l = 0.31$ for helium BI but only 0.17 for nitrogen BI (see Fig. 5).

The tests also showed the dependence of the pressure rise from the injection parameter. For both helium and nitrogen, no further significant pressure rise increases were achieved when the injection parameter was increased above $I_{ax} = 0.03$ for helium injection and $I_{ax} = 0.04$ for nitrogen injection (see Fig. 5). The physical factor leading to this limitation is not understood in detail. It seems that, when the injectant mass flow exceeds a certain level, it is not able to extend the base region further and thereby reduce the corner flow turning angle. This is indicated from the RSP results in Fig. 5, which shows that the RSP approached a limiting position with increasing injection parameter.

The experiments only provide limited data on base pressure rises possible with EB. Further insight into the mixing and combustion processes is necessary to increase the pressure rise. In this study, a pressure rise of $\Delta p_b/p_l = 0.11$ was demonstrated at an injection parameter of $I_{lat} = 0.023$. Tests in Ref. 7 have shown that pressure rises of $\Delta p_b/p_l = 0.22$ are possible if the injection parameter is increased to $I_{lat} = 0.045$.

With the combination of BI and EB, a maximum pressure rise of $\Delta p_b/p_l = 0.42$ was achieved. This is only 70% of the pressure rise needed for the base drag elimination. Higher base pressure can be expected if the pressure rises, which can be achieved independently by EB and/or BI, can be increased. One possibility for increasing the base pressure is the BI of fuels (such as hydrogen or fuel-rich reaction products) to achieve BB. If, with BB, the base pressure can be raised close to freestream pressure, as demonstrated in Ref. 1, then superimposed EB may raise the base pressure above freestream pressure, and a propulsion component could be achieved.

The importance of reactions in the near-wake region, in addition to EB and BI, may be seen from the tests in which BI was combined with EB/BR. In these tests with subsonic lateral injection velocity, the fuel-rich reaction products were probably partly entrained via the projectile boundary into the near-wake region, so that heat addition as well as mass addition from BI occurred. The base pressure achieved in these tests were significantly higher than with combined EB and BI and reached the freestream pressure. It is not clear in these tests, with subsonic lateral injection velocity, whether only base region heating by entrained reaction products and/or combustion of fuel-rich reaction products occurred.

The experimental results described in this paper were achieved in planar, two-dimensional wind tunnel at ambient pressure and Mach 2 flow conditions. It is believed that the trends revealed in this study also will be applicable to other flow conditions and axisymmetric geometries; however, further tests are necessary to substantiate this application.

Conclusions

1) The base pressure rise mechanisms of BI and EB can be superimposed.

2) A base region, which was extended through BI, was compressed by superimposed EB.

3) The base pressure rise with combined EB and BI was nearly the sum of the base pressure rises achieved independently by EB and BI.

4) Base reaction (heating and/or combustion) in addition to EB and BI will increase the base pressure rise further. With this concept, a base pressure equal to freestream pressure was achieved (base drag elimination).

5) The concept of combined EB and BB may provide propulsion, when the base pressure can be raised close to freestream pressure by BB and raised above freestream by EB.

Recommendation

Tests using the 2D, planar wind tunnel have shown that significantly higher base pressures were achieved with combined EB and BI than with EB or BI, independently investigated in the past. The tests also indicated that further base pressure increases may be possible with combined EB and BB. It is recommended that the concepts of combined EB and BI, as well as EB and BB, be investigated in full-scale, axisymmetric wind tunnel tests to determine the specific performance of these concepts.

Acknowledgment

This work was sponsored by the Air Force Office of Scientific Research.

References

[1]Baker, W. T., Davis, T., and Matthews, S. E., "Reduction of Drag on a Projectile in a Supesonic Stream by the Combustion of Hydrogen in the Turbulent Wake," John Hopkins Univ., Applied Physics Lab., CM-673, June 4, 1951.

[2]Townend, L. H. and Reid, J., *Supersonic Flow, Chemical Processes and Radiative Transfer*, Macmillan, New York, 1964, p. 137.

[3]Andersson, K., Gunners, N. E., and Hellgren, R., " 'Swedish Base Bleed'—Increasing the Range of Artillery Projectiles through Base Flow," *Propellants and Explosives*, Vol. 1, 1976, pp. 69-73.

[4]Strahle, W. C., "Theoretical Consideration of Combustion Effects on Base Pressure in Supersonic Flight," *Twelfth Symposium (International) on Combustion*, The Combustion Institute, Pittsburgh, Pa., 1969, p. 1163.

[5]Mehta, G. K. and Strahle, W. C., "A Theory of the Supersonic Turbulent Axisymmetric Near Wake Behind Bluff-Base Bodies," *AIAA Journal*, Vol. 15, Aug. 1977, pp. 1059-1060.

[6]Neale, D. H., Hubbartt, J. E., Strahle, W. C., and Wilson, W. W., "Experiments and Analysis Related to External Burning for Propulsion," Air Force Office of Scientific Research, Washington, D.C., AFOSR-TR-0602, March 1977.

[7]Schadow, K. C. and Chieze, D. J., "Simulation of External Burning in a Two-Dimensional, Planar Wind Tunnel," *14th JANNAF Combustion Conference*, Colorado Springs, Colo., Aug. 15-19, 1977.

[8]Townend, L. H., "Comment on paper by W. C. Strahle, 'Theoretical Consideration of Combustion Effects on Base Pressure in Supersonic Flight,' " *Twelfth Symposium (International) on Combustion*, The Combustion Institute, Pittsburgh, Pa., 1969, p. 1172.